Supplementary Information

High-responsivity Two-dimensional p-PbI_2/n-WS_2 Vertical Heterostructure Photodetectors Enhanced by Photogating Effect

Zhaoyang Qi, Tiefeng Yang, Dong Li, Honglai Li, Xiao Wang, Xuehong Zhang, Fang Li, Weihao Zheng, Peng Fan, Xiujuan Zhuang, Anlian Pan*

Key Laboratory for Micro-Nano Physics and Technology of Hunan Province, College of Materials and Engineering, School of Physics and Electronic Science, and State Key Laboratory of Chemo/Biosensing and Chemometrics, Hunan University, Changsha, Hunan 410082, P. R. China
*Corresponding author: anlian.pan@hnu.edu.cn

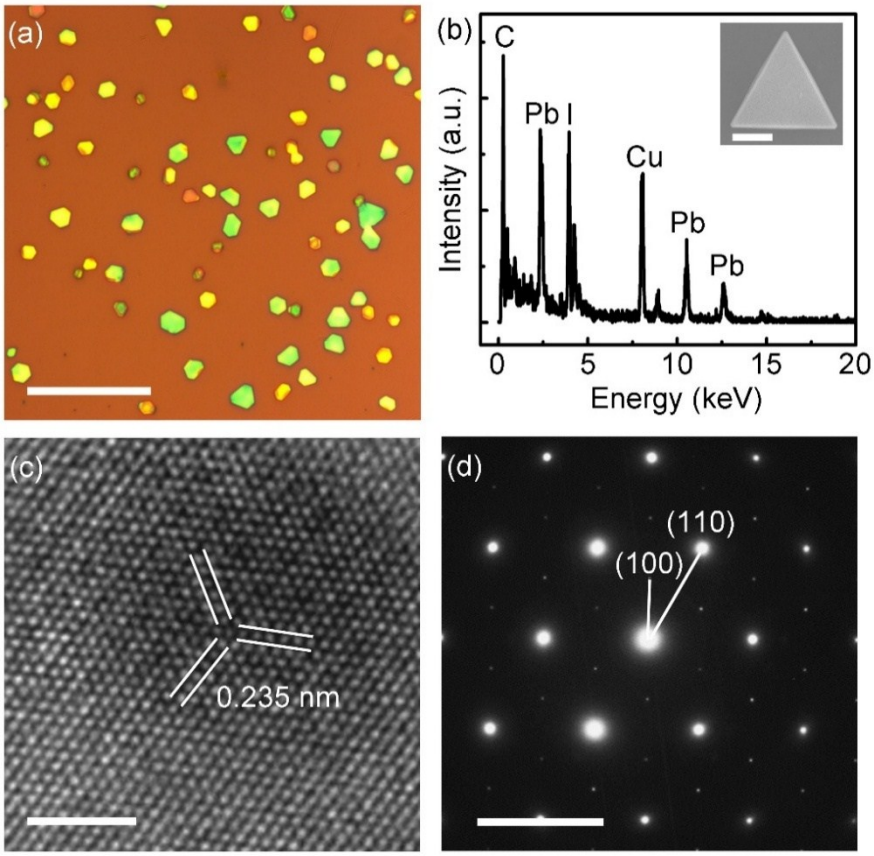

Fig. S1 (a) Optical image of as-grown PbI_2 nanoplates. Scale bar, 20 μm. (b) EDS spectrum collected from a representative nanoplate. Insert is the corresponding SEM image. Scale bar, 200 nm. (c) HRTEM image of PbI_2 nanoplate. The lattice spacings along three different

directions are 0.235 nm, with an intersection angle of 60°. Scale bar, 2 nm. (d) SAED pattern viewed along [001] zone axis. Scale bar, 2 nm^{-1}.

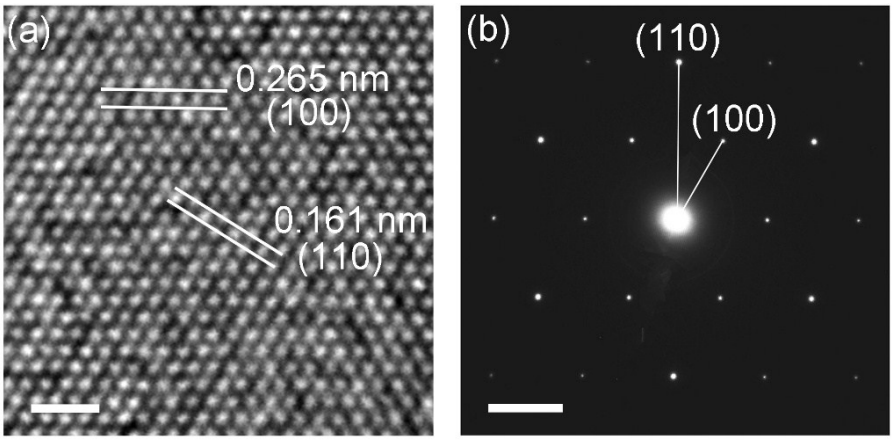

Fig. S2 (a) HRTEM image of monolayer WS_2 transferred on copper grid. (b) SAED pattern viewed along the [001] zone axis. Scale bars, 2 nm, 3 nm^{-1}, respectively.

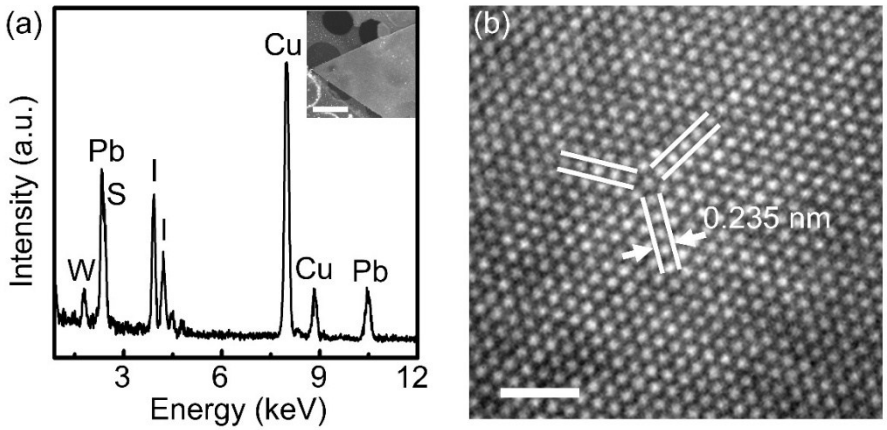

Fig. S3 (a) EDS result of PbI_2/WS_2 nanoplate on copper grid. Inset: low-resolution TEM image. Scale bar: 5 μm. (b) HRTEM image of a typical nanoplate. The interplanar spacings along three directions (marked by yellow lines) are 0.235 nm with an intersection angle of 120°, corresponding to the {110} crystal plane family of PbI_2. Scale bar: 1 nm.

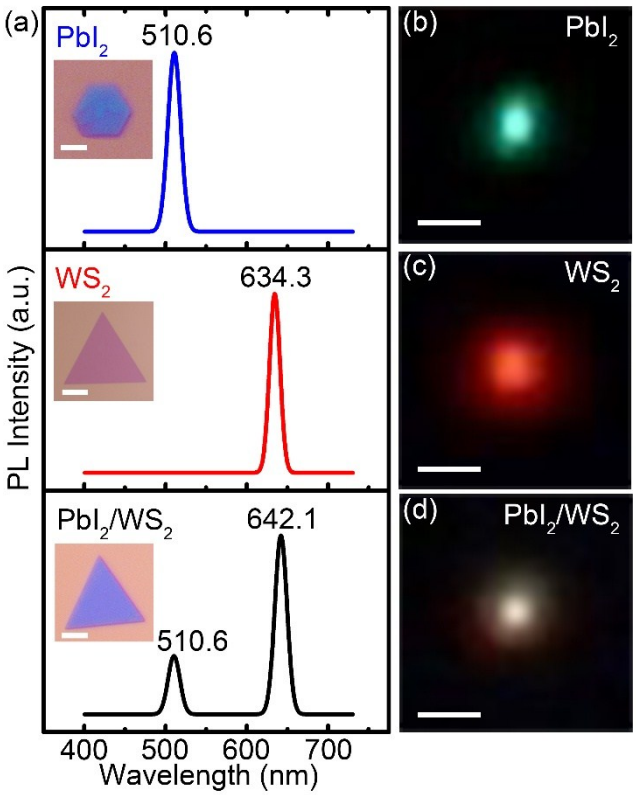

Fig. S4 (a) PL spectra of pristine PbI_2 nanoplate, monolayer WS_2 and PbI_2/WS_2 heterostructure, excited by 450 nm laser. Insert is the corresponding optical images of the measured samples. Scale bars, 2 μm, 5 μm and 5 μm. The real-color PL images are demonstrated in (b-d), respectively. Scale bars, 1 μm.

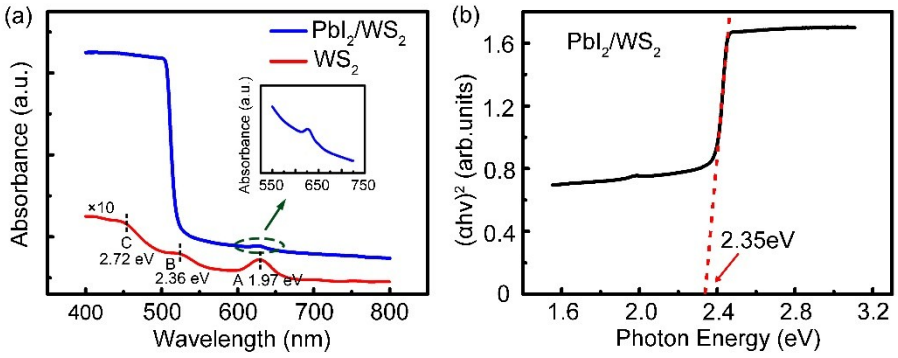

Fig. S5 (a) UV-vis absorption spectra of PbI_2/WS_2 heterostructure and pristine WS_2 (the absorbance intensity of WS_2 is multiplied by 10). The three peaks in the WS_2 absorption spectrum are assigned to A (1.97 eV), B (2.36 eV) and C (2.72 eV) excitonic absorption of pristine WS_2. Insert is the amplification region from PbI_2/WS_2 absorption spectrum. (b) Tauc plot of PbI_2/WS_2 nanoplates absorption spectrum. Bandgap of PbI_2 was deduced to be 2.35 eV from absorbance data using the Tauc relation.[1-3]

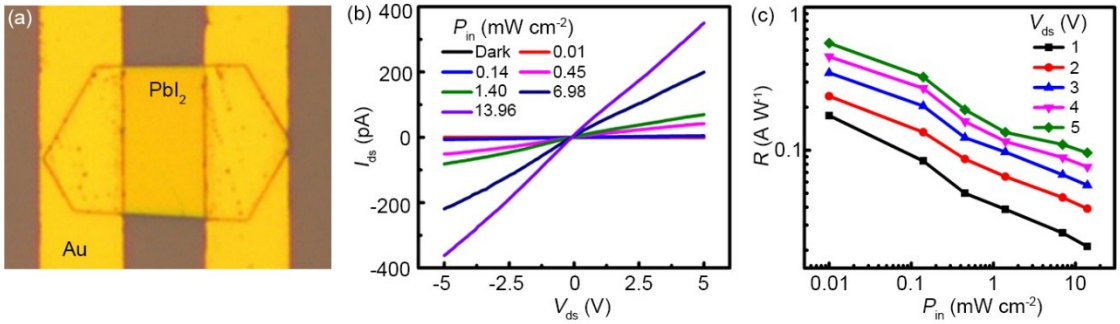

Fig. S6 Optoelectronic characterizations of pristine PbI_2 nanoplate. (a) Optical image of a fabricated PbI_2 device on SiO_2/Si substrate. Scale bar, 5 μm. (b) I_{ds} -V_{ds} curves of the device measured in dark and under various illumination power densities of 450 nm laser (V_{gs} = 0 V). (c) Calculated photoresponsivity as a function of power density at different source-drain voltages.

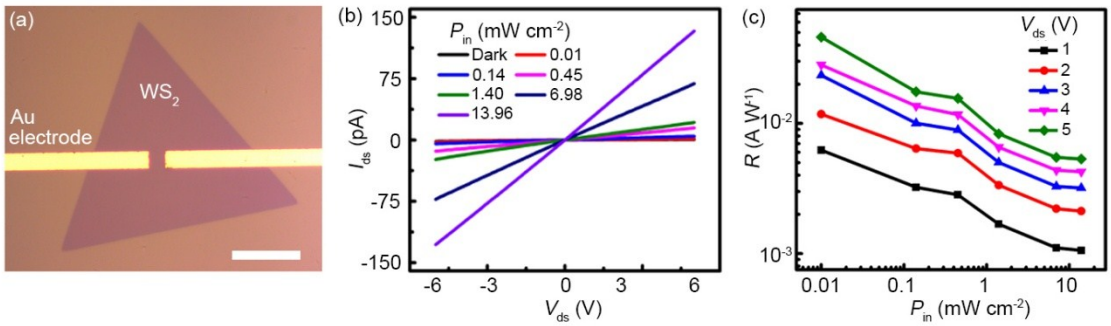

Fig. S7 Optoelectronic performance of monolayer WS_2 nanosheet. (a) Optical image of a representative WS_2 device on SiO_2/Si substrate. Scale bar, 20 μm. (b) I_{ds} -V_{ds} curves of the photodetector measured in dark and under various illumination power densities of 450 nm laser (V_{gs} = 0 V). (c) Extracted photoresponsivity as a function of illumination power density at different source-drain voltages.

Table S1: Comparison with vertical p-n heterostructure and pristine material photodetectors synthesized by CVD method.

Materials	Wavelength [nm]	V_{ds} [V]	V_{gs} [V]	Responsivity [A W^{-1}]	Detectivity [Jones]	Reference
SnS/WS_2	532	1	0	24.2	-	[4]
$GaSe/MoSe_2$	white light	5	0	0.03	-	[5]
WSe_2/SnS_2	520	5	0	0.11	4.71×10^{10}	[6]
$GaSe/MoS_2$	300	1	0	~3.75		[7]
BiI_3/WSe_2	white light	1	0	1.67	-	[8]
ML[a] WS_2	white	20	60	1.88×10^{-2}	-	[9]
FL[b] PbI_2	450	1.9	0	1×10^{-4}	-	[10]
ML WS_2	450	5	0	5.0×10^{-2}	-	This work
FL PbI_2	450	5	0	5.6×10^{-1}	-	This work
PbI_2/WS_2	450	5	0	5.57×10^{2}	6.8×10^{12}	This work
PbI_2/WS_2	450	5	-60	7.1×10^{4}	3.7×10^{13}	This work

[a] ML: monolayer; [b] FL: fewlayer

REFERENCES

1 B. Saparov, F. Hong, J. Sun, H. Duan, W. Meng, S. Cameron, I. G. Hill, Y. Yan and D. B. Mitzi, *Chem. Mater.*, 2015, **27**, 5622-5632.

2 P. Cheng, T. Wu, Y. Li, L. Jiang, W. Deng and K. Han, *New J. Chem.*, 2017, **41**, 9598-9601.

3 M. Leng, Y. Yang, K. Zeng, Z. Chen, Z. Tan, S. Li, J. Li, B. Xu, D. Li, M. P. Hautzinger, Y. Fu, T. Zhai, L. Xu, G. Niu, S. Jin and J. Tang, *Adv. Funct. Mater.*, 2018, **28**, 1704446.

4 A. Sukma Aji, M. Izumoto, K. Suenaga, K. Yamamoto, H. Nakashima and H. Ago, *Phys. Chem. Chem. Phys.*, 2018, **20**, 889-897.

5 X. Li, M.-W. Lin, J. Lin, B. Huang, A. A. Puretzky, C. Ma, K. Wang, W. Zhou, S. T. Pantelides and M. Chi, *Sci. Adv.*, 2016, **2**, e1501882.

6 T. Yang, B. Zheng, Z. Wang, T. Xu, C. Pan, J. Zou, X. Zhang, Z. Qi, H. Liu, Y. Feng, W. Hu, F. Miao, L. Sun, X. Duan and A. Pan, *Nat. Commun.*, 2017, **8**, 1906.

7 N. Zhou, R. Wang, X. Zhou, H. Song, X. Xiong, Y. Ding, J. Lu, L. Gan and T. Zhai, *Small*, 2018, **14**.

8 J. Li, X. Guan, C. Wang, H. C. Cheng, R. Ai, K. Yao, P. Chen, Z. Zhang, X. Duan and X. Duan, *Small*, 2017, **13**.

9 C. Lan, C. Li, Y. Yin and Y. Liu, *Nanoscale*, 2015, **7**, 5974-5980.

10 W. Zheng, Z. Zhang, R. Lin, K. Xu, J. He and F. Huang, *Adv. Electron. Mater.*, 2016, **2**, 1600291.